Available online at www.sciencedirect.com
ScienceDirect
Computer Coupling of Phase Diagrams and Thermochemistry 30 (2006) 449–454
www.elsevier.com/locate/calphad

Activity measurement of the constituents in molten Fe–B and Fe–B–C alloys

Takahiro Miki*, Kenjirou Tsujita[1], Shiro Ban-Ya[2], Mitsutaka Hino

Department of Metallurgy, Graduate School of Engineering, Tohoku University, Aoba-yama 6-6-02, Sendai, 980-8579, Japan

Received 11 April 2006; received in revised form 6 July 2006; accepted 7 July 2006
Available online 17 August 2006

Abstract

The distribution ratios of Fe and B between molten Fe–B alloy and molten Ag were measured at temperatures between 1573 and 1923 K. Also, distribution ratios of Fe and B between molten Fe–B–$C_{satd.}$ alloys and molten Ag were measured at 1873 K. It was found that the excess Gibbs free energy of mixing in molten Fe–B and Fe–B–C alloys can be expressed by utilizing the Redlich–Kister polynomial. The activity curves of the elements in molten Fe–B alloy and Fe–B–C alloy were estimated.

Keywords: Activity; Equilibrium; Excess Gibbs free energy; Redlich–Kister polynomial

1. Introduction

Boron is used as an alloying element to enhance the hardness of steel. This is mainly due to the segregation of B, the austenite grain boundaries, and suppression of the enlargement of primary ferrite formation. Also, the Fe–B binary is the basic system of ferrous amorphous alloys. Therefore, it is important to understand the thermodynamic behavior of B in Fe- based alloys. The phase diagram of the Fe–B system [1] has been reported, as shown in Fig. 1. Thermodynamic evaluations and measurements of the Fe–B binary system [1–5] and the Fe–B–C ternary system [6,7] have been reported by several researchers. However, direct activity measurements of the constituents in molten Fe–B binary and Fe–B–C ternary alloys have not been reported. Accurate activity information of the constituents in these alloys will be indispensable for any high-precision thermodynamic assessment of the Fe–B binary and Fe–B–C ternary systems.

In the present work, the distribution ratios of Fe and B between molten Fe–B alloys, Fe–B–$C_{satd.}$ alloys, and molten Ag were measured at temperatures between 1573–1923 K and 1873 K, respectively. Although the presence of AgB_2 is reported [8], Ag and B are, essentially, mutually insoluble in their solid and liquid states. The temperature dependence of the solubility of Fe in molten Ag was determined from the present experimental results. The activity of Fe in Fe–B alloys was determined utilizing the Fe distribution results and the results about Fe solubility in molten Ag. The activity of B in Fe–B binary alloys was obtained by using the Gibbs–Duhem equation. The excess Gibbs free energy of the molten Fe–B–C system at 1873 K was determined from the present results by utilizing the Redlich–Kister polynomial, and the activity curves of the constituents was thereby obtained.

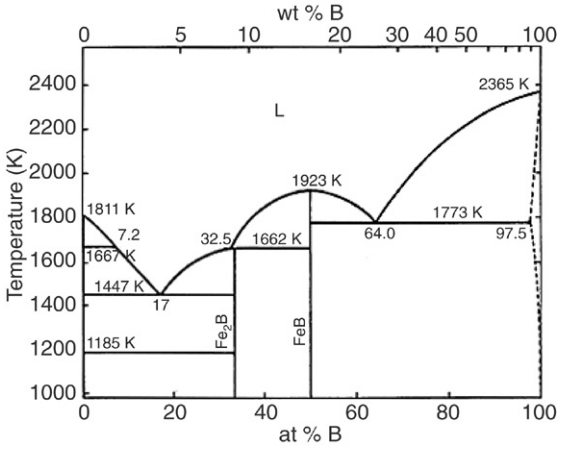

Fig. 1. Phase diagram of Fe–B system [1].

* Corresponding author. Tel.: +81 22 795 7307; fax: +81 22 795 7307.
E-mail address: miki@material.tohoku.ac.jp (T. Miki).
[1] Formerly Graduate Student, Tohoku University, now Fujilight Carpet Co., Ltd.
[2] Emeritus Professor, Tohoku University.

0364-5916/$ - see front matter © 2006 Published by Elsevier Ltd
doi:10.1016/j.calphad.2006.07.001

Table 1
Experimental results of Fe and B distributions between the molten Fe–B and Ag phases

T (K)	$X_B^{(Fe)}$	$X_B^{(Ag)} \times 10^4$	$X_{Fe}^{(Ag)} \times 10^3$	$a_{Fe(l)}$
1923	0.030	–	7.90	0.961
1923	0.052	–	7.30	0.889
1923	0.064	–	7.31	0.890
1923	0.102	–	6.56	0.799
1923	0.206	0.084	4.38	0.533
1923	0.296	0.171	3.81	0.464
1923	0.403	0.392	2.21	0.269
1923	0.584	0.772	0.347	0.042
1923	0.636	1.04	0.224	0.027
1873	0.025	–	7.34	0.969
1873	0.050	–	6.65	0.879
1873	0.071	–	6.40	0.846
1873	0.086	–	5.83	0.771
1873	0.143	–	4.85	0.641
1873	0.193	0.043	4.07	0.538
1873	0.239	0.092	4.05	0.535
1873	0.295	0.118	3.67	0.485
1873	0.341	0.233	2.97	0.392
1873	0.398	0.275	2.28	0.301
1873	0.432	0.546	1.87	0.247
1873	0.596	1.03	0.244	0.032
1873	0.607	1.04	0.205	0.027
1873	0.622	1.50	0.247	0.033
1873	0.639	1.54	0.184	0.024
1773	0.102	–	4.96	0.805
1773	0.145	–	4.23	0.687
1773	0.194	–	3.18	0.517
1773	0.247	0.077	2.73	0.443
1773	0.300	0.062	2.93	0.476
1773	0.344	0.097	2.16	0.350
1773	0.374	0.212	1.69	0.274

2. Experimental set-up

An electric resistance furnace was used for equilibrating the experiment. The temperature was controlled by a Pt-6%Rh/Pt-30%Rh thermocouple. Weights of 6–8 g of Fe–B alloy and 8 g of Ag were set in an alumina crucible or graphite crucible and placed in the hot zone of the furnace. The samples were equilibrated under a purified Ar flow for 12 h. This experimental time was confirmed to be sufficient for the preliminary experiment. After keeping the sample in the furnace for a given period, it was quenched by withdrawing it from the furnace and dipping it into water, and supplying it for chemical analysis. The B and Fe contents in the Ag phase, and B content in the Fe–B(–C) phase, were determined by inductively coupled plasma spectroscopy (ICP). The content of C in the Fe–B–C phase was analyzed by the combustion gravimetric method.

3. Experimental results

The experimental results of the B and Fe distributions between molten Fe–B alloy and molten Ag phases are shown in Table 1. The relationship between B content in Fe–B alloy and that in Ag is shown in Fig. 2. The content of B was lower than 25 ppm. The temperature dependence on the B distribution

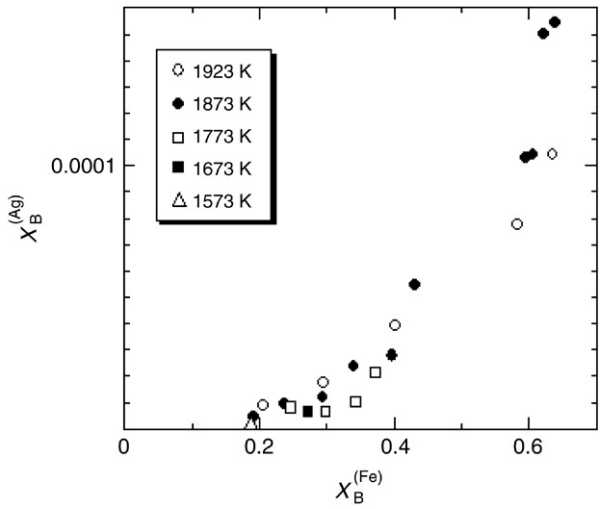

Fig. 2. Relationship between B contents in the Fe–B phase and that of the Ag phase.

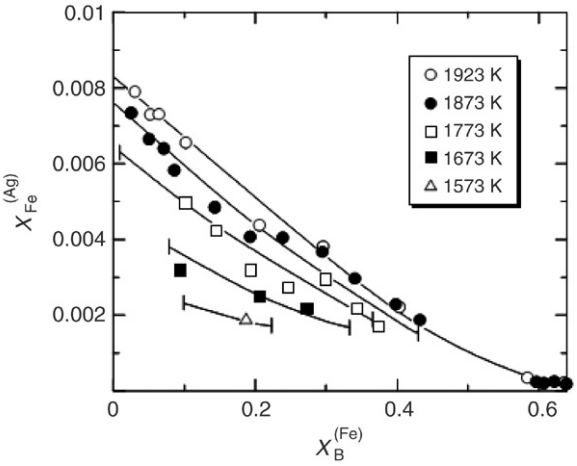

Fig. 3. Relationship between B contents in the Fe–B phase and Fe contents in the Ag phase.

between a molten Fe–B alloy and molten Ag was negligible. The relationship between Fe content in an Fe–B alloy and that in Ag is shown in Fig. 3. The equilibrium Fe content in Ag decreased with the increase of B content in an Fe–B alloy. The Fe–B alloy in Fig. 3 was in the liquid phase, not a mixture of solid and liquid, according to the Fe–B phase diagram. Hence, the curves in Fig. 3 were determined from the results taking into account the scatter of experimental data.

The experimental results of B and Fe distributions between C- saturated molten Fe–B–C alloy and molten Ag are shown in Table 2 and Fig. 4. It was impossible to analyze the B content of Ag for a few samples due to low B concentration.

It was found that an increase of B will decrease the C solubility in Fe–B–C alloy.

4. Discussion

4.1. Activities of the constituents in molten Fe–B binary alloy

The chemical potential or activity of Fe in the molten Fe–B phase and the Ag phase is equivalent at equilibrium. The

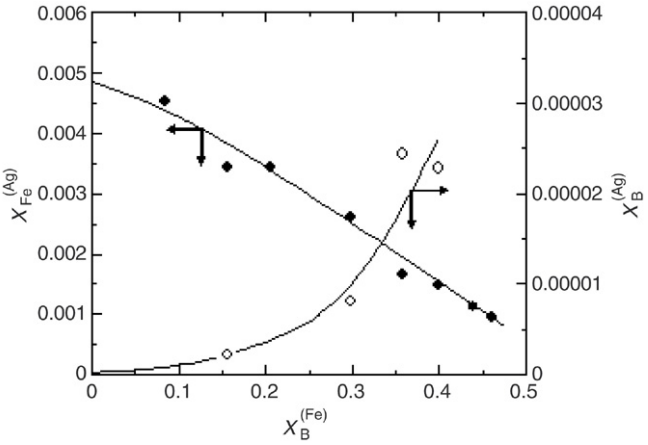

Fig. 4. Relationship between B contents in the Fe–B–$C_{satd.}$ phase and B, Fe contents in the Ag phase at 1873 K.

Table 2
Experimental results of Fe and B distribution between molten Fe–B–C and Ag phases at 1873 K

$X_B^{(Fe)}$	$X_C^{(Fe)}$	$X_B^{(Ag)} \times 10^4$	$X_{Fe}^{(Ag)} \times 10^3$	$\gamma_{C(s)}^{(Fe)}$	$a_{Fe(l)}$
0.046	0.172	–	–	5.81	–
0.084	0.146	–	4.53	6.85	0.598
0.156	0.123	0.022	3.43	8.13	0.453
0.205	0.097	–	3.45	10.3	0.456
0.299	0.051	0.081	2.61	19.6	0.345
0.357	0.039	0.244	1.67	25.6	0.221
0.399	0.027	0.228	1.5	37.0	0.199
0.439	0.028	–	1.12	35.7	0.148
0.461	0.016	–	0.942	62.5	0.124

activity of Fe is unity when the Ag phase is saturated with Fe. It can be assumed that Fe in the Ag phase obeys Henry's law, because the Fe content in the Ag phase is extremely low. Hence, the activity of Fe in an Fe–B alloy can be obtained from the following relation.

$$a_{Fe(l)}^{(Fe)} = \frac{X_{Fe}^{(Ag)}}{X_{Fe(satd.)}^{(Ag)}}. \quad (1)$$

Here, $a_{Fe(l)}^{(Fe)}$ is the activity of Fe in an Fe-rich phase with reference to pure liquid Fe, $X_{Fe}^{(Ag)}$ is mole fraction of Fe in the Ag phase, and $X_{Fe(satd.)}^{(Ag)}$ is the solubility limit of Fe in the Ag phase. The results of Kimoto et al. [9] were utilized for the solubility limit of Fe in the Ag phase. Fe activity as determined by Eq. (1) is shown in Tables 1 and 2.

The relation of $(1 - X_{Fe})^2$ and $RT \ln \gamma_{Fe(l)}^{(Fe)}$ for an Fe–B binary alloy is shown in Fig. 5. Here R, T and $\gamma_{Fe(l)}^{(Fe)}$ are the gas constant, absolute temperature, and activity of Fe(l) in the Fe phase, respectively. Temperature dependence in Fig. 5 could not be observed. The activity coefficient of Fe in an Fe–B binary alloy, $RT \ln \gamma_{Fe(l)}^{(Fe)}/(\mathrm{J\,mol^{-1}})$, can be expressed by the following equation.

$$RT \ln \gamma_{Fe(l)}^{(Fe)} = -76\,300(1 - X_{Fe})^2 - 71\,720(1 - X_{Fe})^4. \quad (2)$$

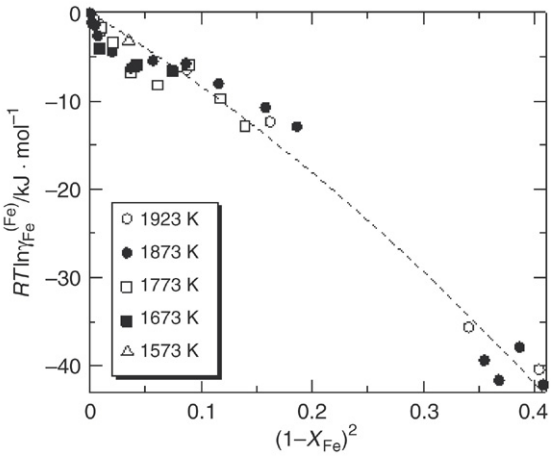

Fig. 5. Relationship between $(1 - X_{Fe})^2$ and $RT \ln \gamma_{Fe(l)}^{(Fe)}$.

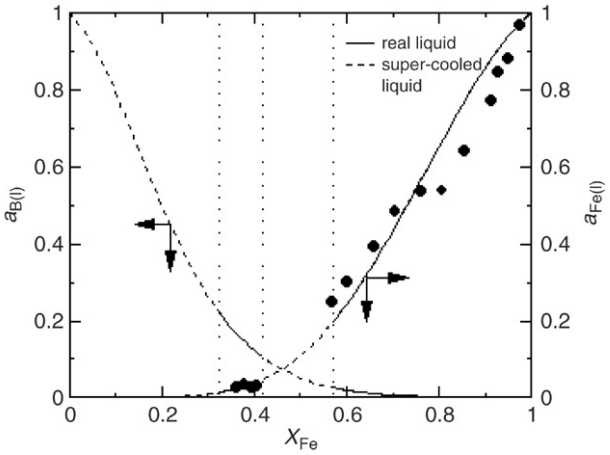

Fig. 6. The activity curves of Fe and B in an Fe–B binary system at 1873 K. Standard state: pure liquid substance.

The activity of B in an Fe–B binary alloy can be obtained from the following Gibbs–Duhem equation.

$$X_B \mathrm{d} \ln \gamma_{B(l)}^{(Fe)} + X_{Fe} \mathrm{d} \ln \gamma_{Fe(l)}^{(Fe)} = 0. \quad (3)$$

Eq. (3) can be rearranged as Eq. (4) as follows.

$$RT \ln \gamma_{B(l)}^{(Fe)} = -\int_{X_B=1}^{X_B} \frac{X_{Fe}}{X_B} \mathrm{d}(RT \ln \gamma_{Fe(l)}^{(Fe)}). \quad (4)$$

The activity coefficient of B in an Fe–B binary alloy with reference to pure molten B, $RT \ln \gamma_{B(l)}^{(Fe)}/(\mathrm{J\ mol^{-1}})$, is determined as follows.

$$RT \ln \gamma_{B(l)}^{(Fe)} = -100\,200 + 152\,700X_B - 76\,330X_B^2 + 95\,630X_B^3 - 71\,720X_B^4. \quad (5)$$

The activities of Fe and B in a molten Fe–B binary alloy at 1873 K are shown in Fig. 6, where the Fe activity reported has been obtained from the experimental results. The activities show a negative deviation from the ideal behavior. The activity coefficient of B in an infinitely dilute molten Fe–B alloy with reference to pure molten B, $\gamma_{B(l)}^{\circ(Fe)}$, can be determined as 0.00160 at 1873 K.

Table 3
Comparison of $\gamma^{\circ(\mathrm{Fe})}_{\mathrm{B(s)}}$ and $\varepsilon^{\mathrm{B(Fe)}}_{\mathrm{B}}$

Author(s)	$\varepsilon^{\mathrm{B(Fe)}}_{\mathrm{B}}$	$\gamma^{\circ(\mathrm{Fe})}_{\mathrm{B(s)}}$	T (K)
Schenck et al.	1.52 ($X_{\mathrm{B}} < 0.25$) 9.3 ($X_{\mathrm{B}} > 0.25$)	0.64	1873
Ball et al.	3.67	0.018	1873
Evans et al.	2.5	0.022	1823
Fruehan	–	0.083	1823
Elliott et al.	5.8	0.022	1873
Ji et al.	5.7	0.041	1723
Present authors	9.80	0.00306	1873

By utilizing the Gibbs free energy change [10] of the B fusion reaction, $\Delta G^{\circ}_{\mathrm{fus.}}$/J, the activity coefficient of B in an infinitely dilute molten Fe–B alloy with reference to pure solid B, $\gamma^{\circ(\mathrm{Fe})}_{\mathrm{B(s)}}$, can be determined as 0.00306 at 1873 K.

$$\mathrm{B(s)} = \mathrm{B(l)} \qquad \Delta G^{\circ}_{\mathrm{fus.}} = 49\,070 - 20.81T \tag{6}$$

$$a_{\mathrm{B(s)}}/a_{\mathrm{B(l)}} = 1.91\ (1873\ \mathrm{K}). \tag{7}$$

Also, the first order interaction parameter, $\varepsilon^{\mathrm{B}}_{\mathrm{B}}$, at 1873 K can be calculated as 9.80. These values are compared with the results reported by other researchers [11–16] in Table 3. The activity coefficient of B in an infinitely dilute molten Fe–B alloy with reference to pure solid B, as determined in the present work, was found to be smaller than the values reported in the literature.

The excess Gibbs free energy of mixing for an Fe–B binary alloy, $\Delta G^{\mathrm{ex}}_{\mathrm{M(Fe–B)}}$, can be determined from the following equation.

$$\Delta G^{\mathrm{ex}}_{\mathrm{M(Fe–B)}} = RTX_{\mathrm{Fe}} \ln \gamma^{(\mathrm{Fe})}_{\mathrm{Fe(l)}} + RTX_{\mathrm{B}} \ln \gamma^{(\mathrm{Fe})}_{\mathrm{B(l)}}. \tag{8}$$

From Eqs. (2), (5) and (8), $\Delta G^{\mathrm{ex}}_{\mathrm{M(Fe–B)}}$/J can be determined utilizing a Redlich–Kister type polynomial [17,18] at temperatures between 1573 and 1923 K.

$$\begin{aligned}\Delta G^{\mathrm{ex}}_{\mathrm{M(Fe–B)}} = {} & X_{\mathrm{Fe}}X_{\mathrm{B}}\{-118\,200 + 23\,910(X_{\mathrm{Fe}} - X_{\mathrm{B}}) \\ & - 5980(X_{\mathrm{Fe}} - X_{\mathrm{B}})^2\}.\end{aligned} \tag{9}$$

The $\Delta G^{\mathrm{ex}}_{\mathrm{M(Fe–B)}}$ determined in the present work was more negative than that assessed by Hallemans et al. [3].

4.2. Activities of the constituents in molten Fe–B–C ternary alloy

The excess Gibbs free energy change of mixing for an Fe–B–C ternary alloy, $\Delta G^{\mathrm{ex}}_{\mathrm{M(Fe–B–C)}}$/J, can be shown utilizing a Redlich–Kister type polynomial as follows.

$$\begin{aligned}\Delta G^{\mathrm{ex}}_{\mathrm{M(Fe–B–C)}} = {} & X_{\mathrm{Fe}}X_{\mathrm{B}}\{{}^0\Omega_{\mathrm{Fe–B}} + {}^1\Omega_{\mathrm{Fe–B}}(X_{\mathrm{Fe}}–X_{\mathrm{B}}) \\ & + {}^2\Omega_{\mathrm{Fe–B}}(X_{\mathrm{Fe}} - X_{\mathrm{B}})^2\} \\ & + X_{\mathrm{Fe}}X_{\mathrm{C}}\{{}^0\Omega_{\mathrm{Fe–C}} + {}^1\Omega_{\mathrm{Fe–C}}(X_{\mathrm{Fe}} - X_{\mathrm{C}}) \\ & + {}^2\Omega_{\mathrm{Fe–C}}(X_{\mathrm{Fe}} - X_{\mathrm{C}})^2\} \\ & + X_{\mathrm{B}}X_{\mathrm{C}}\{{}^0\Omega_{\mathrm{B–C}} + {}^1\Omega_{\mathrm{B–C}}(X_{\mathrm{B}} - X_{\mathrm{C}})\}.\end{aligned} \tag{10}$$

Ω_{i-j} is the binary interaction parameter. The ternary interaction parameter $\Omega_{\mathrm{Fe–B–C}}$ is assumed to be negligible in the present work. The standard states of Fe and B are pure liquid. Liquid that equilibrates with solid C was chosen as the standard state of C. However, there is a concentration limit that Eq. (9) can be utilized.

The excess Gibbs free energy change of mixing for an Fe–C binary alloy, $\Delta G^{\mathrm{ex}}_{\mathrm{M(Fe–C)}}$/J, at 1873 K can be determined as Eq. (10) from the evaluated Gibbs energy change of liquid C to solid C and parameters assessed by Ohtani et al. [19]

$$\begin{aligned}\Delta G^{\mathrm{ex}}_{\mathrm{M(Fe–C)}} = {} & X_{\mathrm{Fe}}X_{\mathrm{C}}\{68\,470 - 126\,000(X_{\mathrm{Fe}} - X_{\mathrm{C}}) \\ & + 50\,960(X_{\mathrm{Fe}} - X_{\mathrm{C}})^2\}.\end{aligned} \tag{11}$$

The unknown parameters in Eq. (10) will be ${}^0\Omega_{\mathrm{B–C}}$ and ${}^1\Omega_{\mathrm{B–C}}$ utilizing Eqs. (9) and (11). Ansara et al. [20] have assessed $\Omega_{\mathrm{B–C}}$ from the B–C phase diagram. The liquid phase of B–C binary system appears at temperatures higher than 2350 K, which is much higher than those used in the present work. Hence, $\Omega_{\mathrm{B–C}}$ as assessed by Ansara et al. [20] was not utilized in the present work. The activity coefficient of C in a molten Fe–B–C ternary alloy $RT \ln \gamma^{(\mathrm{Fe–B–C})}_{\mathrm{C(s)}}$/(J mol^{-1}) can be expressed by the following equation.

$$\begin{aligned}\Delta \overline{G}^{\mathrm{ex}}_{\mathrm{C}} = {} & RT \ln \gamma^{(\mathrm{Fe–B–C})}_{\mathrm{C(s)}} = \Delta G^{\mathrm{ex}}_{\mathrm{M(Fe–B–C)}} \\ & - X_{\mathrm{Fe}} \frac{\partial \Delta G^{\mathrm{ex}}_{\mathrm{M(Fe–B–C)}}}{\partial X_{\mathrm{Fe}}} - X_{\mathrm{B}} \frac{\partial \Delta G^{\mathrm{ex}}_{\mathrm{M(Fe–B–C)}}}{\partial X_{\mathrm{B}}} \\ = {} & -X_{\mathrm{Fe}}X_{\mathrm{B}}\{{}^0\Omega_{\mathrm{Fe–B}} + 2 \cdot {}^1\Omega_{\mathrm{Fe–B}}(X_{\mathrm{Fe}} - X_{\mathrm{B}}) \\ & + 3 \cdot {}^2\Omega_{\mathrm{Fe–B}}(X_{\mathrm{Fe}} - X_{\mathrm{B}})^2\} \\ & + X_{\mathrm{Fe}}(1 - X_{\mathrm{C}})\{{}^0\Omega_{\mathrm{Fe–C}} + {}^1\Omega_{\mathrm{Fe–C}}(X_{\mathrm{Fe}} - X_{\mathrm{C}}) \\ & + {}^2\Omega_{\mathrm{Fe–C}}(X_{\mathrm{Fe}} - X_{\mathrm{C}})^2\} \\ & + X_{\mathrm{Fe}}X_{\mathrm{C}}(-1 - X_{\mathrm{Fe}} + X_{\mathrm{C}})\{{}^1\Omega_{\mathrm{Fe–C}} \\ & + 2 \cdot {}^2\Omega_{\mathrm{Fe–C}}(X_{\mathrm{Fe}} - X_{\mathrm{C}})\} \\ & + X_{\mathrm{B}}(1 - X_{\mathrm{C}})\{{}^0\Omega_{\mathrm{B–C}} + {}^1\Omega_{\mathrm{B–C}}(X_{\mathrm{B}} - X_{\mathrm{C}})\} \\ & + X_{\mathrm{B}}X_{\mathrm{C}}(-1 - X_{\mathrm{B}} + X_{\mathrm{C}})\,{}^1\Omega_{\mathrm{B–C}}.\end{aligned} \tag{12}$$

The following equation can be derived by rearranging Eq. (12).

$$\begin{aligned}F = {} & \frac{1}{X_{\mathrm{B}}(1 - X_{\mathrm{C}})}\{X_{\mathrm{Fe}}X_{\mathrm{B}}\{{}^0\Omega_{\mathrm{Fe–B}} + 2 \cdot {}^1\Omega_{\mathrm{Fe–B}}(X_{\mathrm{Fe}} - X_{\mathrm{B}}) \\ & + 3 \cdot {}^2\Omega_{\mathrm{Fe–B}}(X_{\mathrm{Fe}} - X_{\mathrm{B}})^2\} \\ & - X_{\mathrm{Fe}}(1 - X_{\mathrm{C}})\{{}^0\Omega_{\mathrm{Fe–C}} + {}^1\Omega_{\mathrm{Fe–C}}(X_{\mathrm{Fe}} - X_{\mathrm{C}}) \\ & + {}^2\Omega_{\mathrm{Fe–C}}(X_{\mathrm{Fe}} - X_{\mathrm{C}})^2\} \\ & - X_{\mathrm{Fe}}X_{\mathrm{C}}(-1 - X_{\mathrm{Fe}} + X_{\mathrm{C}})\{{}^1\Omega_{\mathrm{Fe–C}} \\ & + 2 \cdot {}^2\Omega_{\mathrm{Fe–C}}(X_{\mathrm{Fe}} - X_{\mathrm{C}})\} + RT \ln \gamma^{(\mathrm{Fe–B–C})}_{\mathrm{C(s)}}\} \\ = {} & {}^0\Omega_{\mathrm{B–C}} + {}^1\Omega_{\mathrm{B–C}} \frac{X_{\mathrm{B}} - 2X_{\mathrm{C}} - 2X_{\mathrm{B}}X_{\mathrm{C}} + 2X_{\mathrm{C}}^2}{1 - X_{\mathrm{C}}}.\end{aligned} \tag{13}$$

The left hand side of Eq. (13), F/J, can be estimated from the activity coefficient of C in Fe–B–C ternary alloys as determined in the present work Eqs. (9) and (11). The unknown parameters

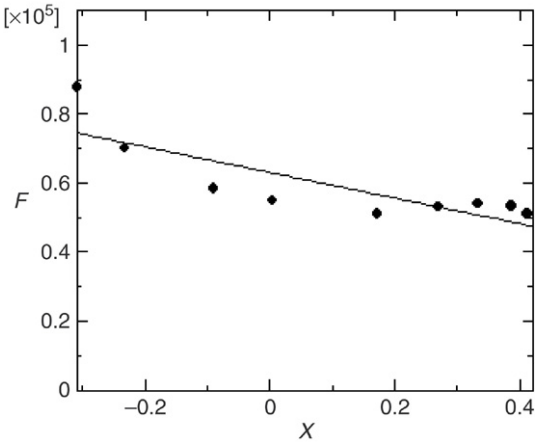

Fig. 7. Determination of ${}^0\Omega_{\mathrm{B-C}}$ and ${}^1\Omega_{\mathrm{B-C}}$ at 1873 K.

${}^0\Omega_{\mathrm{B-C}}$ and ${}^1\Omega_{\mathrm{B-C}}$ can be obtained from the intercept and the slope of the graph by taking the left hand side of Eq. (13) as the vertical axis and $X = \frac{X_B - 2X_C - 2X_B X_C + 2X_C^2}{1 - X_C}$ as the horizontal axis. The result is shown in Fig. 7. Therefore, ${}^0\Omega_{\mathrm{B-C}}$ /J and ${}^1\Omega_{\mathrm{B-C}}$ /J are estimated as follows from Fig. 7.

$${}^0\Omega_{\mathrm{B-C}} = 63\,010$$
$${}^1\Omega_{\mathrm{B-C}} = -37\,050.$$

The excess Gibbs free energy change of mixing for a B–C binary, $\Delta G^{\mathrm{ex}}_{\mathrm{M(B-C)}}$/J, at 1873 K was determined as follows.

$$\Delta G^{\mathrm{ex}}_{\mathrm{M(B-C)}} = X_B X_C\{63\,010 - 37\,050(X_B - X_C)\}. \quad (14)$$

The binary interaction parameters determined and utilized are summarized in Table 4. The activities of the constituents in a molten Fe–B–C ternary alloy at 1873 K obtained by Eqs. (12), (15) and (16) are shown in Figs. 8–10.

$$\begin{aligned}
\Delta\overline{G}^{\mathrm{ex}}_{\mathrm{Fe}} &= RT\ln\gamma^{(\mathrm{Fe-B-C})}_{\mathrm{Fe(l)}} \\
&= \Delta G^{\mathrm{ex}}_{\mathrm{M(Fe-B-C)}} - X_B\frac{\partial\Delta G^{\mathrm{ex}}_{\mathrm{M(Fe-B-C)}}}{\partial X_B} \\
&\quad - X_C\frac{\partial\Delta G^{\mathrm{ex}}_{\mathrm{M(Fe-B-C)}}}{\partial X_C} \\
&= (1-X_{\mathrm{Fe}})X_B\{{}^0\Omega_{\mathrm{Fe-B}} + {}^1\Omega_{\mathrm{Fe-B}}(X_{\mathrm{Fe}} - X_B) \\
&\quad + {}^2\Omega_{\mathrm{Fe-B}}(X_{\mathrm{Fe}} - X_B)^2\} \\
&\quad + X_{\mathrm{Fe}}X_B(1 - X_{\mathrm{Fe}} + X_B)\{{}^1\Omega_{\mathrm{Fe-B}} \\
&\quad + 2\cdot{}^2\Omega_{\mathrm{Fe-B}}(X_{\mathrm{Fe}} - X_B)\} \\
&\quad + (1-X_{\mathrm{Fe}})X_C\{{}^0\Omega_{\mathrm{Fe-C}} + {}^1\Omega_{\mathrm{Fe-C}}(X_{\mathrm{Fe}} - X_C) \\
&\quad + {}^2\Omega_{\mathrm{Fe-C}}(X_{\mathrm{Fe}} - X_C)^2\} \\
&\quad + X_{\mathrm{Fe}}X_C(1 - X_{\mathrm{Fe}} + X_C)\{{}^1\Omega_{\mathrm{Fe-C}} \\
&\quad + 2\cdot{}^2\Omega_{\mathrm{Fe-C}}(X_{\mathrm{Fe}} - X_C)\} \\
&\quad - X_B X_C\{{}^0\Omega_{\mathrm{B-C}} + 2\cdot{}^1\Omega_{\mathrm{B-C}}(X_B - X_C)\} \quad (15)
\end{aligned}$$

Table 4
Summarized binary interaction parameters at 1873 K

Binary interaction parameter	Value (J)
${}^0\Omega_{\mathrm{Fe-B}}$	−118 200
${}^1\Omega_{\mathrm{Fe-B}}$	23 910
${}^2\Omega_{\mathrm{Fe-B}}$	−5 980
${}^0\Omega_{\mathrm{Fe-C}}$	68 470
${}^1\Omega_{\mathrm{Fe-C}}$	−126 000
${}^2\Omega_{\mathrm{Fe-C}}$	50 960
${}^0\Omega_{\mathrm{B-C}}$	63 010
${}^1\Omega_{\mathrm{B-C}}$	−37 050

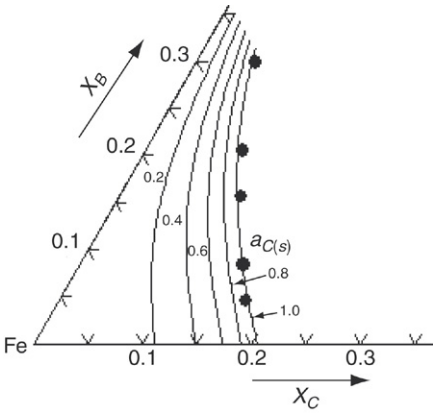

Fig. 8. Iso-activity curve of C in a molten Fe–B–C system at 1873 K. Standard state : C(s).

$$\begin{aligned}
\Delta\overline{G}^{\mathrm{ex}}_{\mathrm{B}} &= RT\ln\gamma^{(\mathrm{Fe-B-C})}_{\mathrm{B(l)}} \\
&= \Delta G^{\mathrm{ex}}_{\mathrm{M(Fe-B-C)}} - X_{\mathrm{Fe}}\frac{\partial\Delta G^{\mathrm{ex}}_{\mathrm{M(Fe-B-C)}}}{\partial X_{\mathrm{Fe}}} \\
&\quad - X_C\frac{\partial\Delta G^{\mathrm{ex}}_{\mathrm{M(Fe-B-C)}}}{\partial X_C} \\
&= X_{\mathrm{Fe}}(1-X_B)\{{}^0\Omega_{\mathrm{Fe-B}} + {}^1\Omega_{\mathrm{Fe-B}}(X_{\mathrm{Fe}} - X_B) \\
&\quad + {}^2\Omega_{\mathrm{Fe-B}}(X_{\mathrm{Fe}} - X_B)^2\} \\
&\quad + X_{\mathrm{Fe}}X_B(-1 - X_{\mathrm{Fe}} + X_B)\{{}^1\Omega_{\mathrm{Fe-B}} \\
&\quad + 2\cdot{}^2\Omega_{\mathrm{Fe-B}}(X_{\mathrm{Fe}} - X_B)\} \\
&\quad - X_{\mathrm{Fe}}X_C\{{}^0\Omega_{\mathrm{Fe-C}} + 2\cdot{}^1\Omega_{\mathrm{Fe-C}}(X_{\mathrm{Fe}} - X_C) \\
&\quad + 3\cdot{}^2\Omega_{\mathrm{Fe-C}}(X_{\mathrm{Fe}} - X_C)^2\} \\
&\quad + (1-X_B)X_C\{{}^0\Omega_{\mathrm{B-C}} + {}^1\Omega_{\mathrm{B-C}}(X_B - X_C)\} \\
&\quad + X_B X_C(1 - X_B + X_C)\,{}^1\Omega_{\mathrm{B-C}}. \quad (16)
\end{aligned}$$

The C solubility at 1873 K obtained in the present work agreed with that determined from the assessed values in previous results [6,7]. However, the determined iso-activity curve of B differs from the previous results [6,7].

5. Conclusion

The excess Gibbs free energy of mixing for a molten Fe–B binary alloy at temperatures between 1573 and 1923 K was determined as follows. The standard state of Fe and B are pure liquid.

$$\Delta G^{\mathrm{ex}}_{\mathrm{M(Fe-B)}}/\mathrm{J} = X_{\mathrm{Fe}}X_B\{-118\,200 + 23\,910(X_{\mathrm{Fe}} - X_B) - 5980(X_{\mathrm{Fe}} - X_B)^2\}.$$

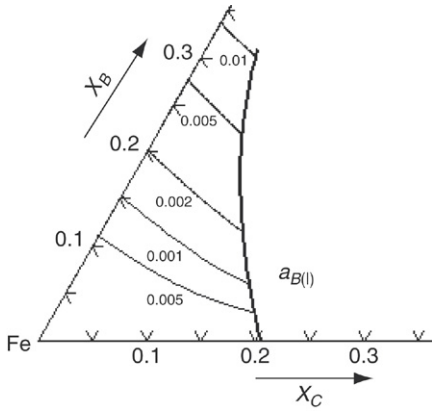

Fig. 9. Iso-activity curve of B in a molten Fe–B–C system at 1873 K. Standard state: B(l).

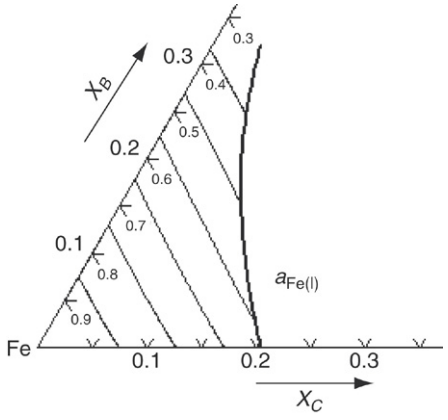

Fig. 10. Iso-activity curve of Fe in a molten Fe–B–C system at 1873 K. Standard state: Fe(l).

Also, the excess Gibbs free energy of mixing for a molten Fe–B–C ternary alloy at 1873 K was determined as follows. Liquid that equilibrates with solid C was chosen as a standard state of C.

$$\begin{aligned}\Delta G^{\mathrm{ex}}_{\mathrm{M(Fe\text{–}B\text{–}C)}}/\mathrm{J} = {} & X_{\mathrm{Fe}}X_{\mathrm{B}}\{-118\,200 + 23\,910(X_{\mathrm{Fe}} - X_{\mathrm{B}}) \\ & - 5980(X_{\mathrm{Fe}} - X_{\mathrm{B}})^2\} \\ & + X_{\mathrm{Fe}}X_{\mathrm{C}}\{68\,470 - 126\,000(X_{\mathrm{Fe}} - X_{\mathrm{C}}) \\ & + 50\,960(X_{\mathrm{Fe}} - X_{\mathrm{C}})^2\} \\ & + X_{\mathrm{B}}X_{\mathrm{C}}\{63\,010 - 37\,050(X_{\mathrm{B}} - X_{\mathrm{C}})\}.\end{aligned}$$

The activity curves of the elements in a molten Fe–B alloy and iso-activity curves of the elements in a molten Fe–B–C alloy were determined.

References

[1] T.B. Massalski (Ed.), Binary Alloys Phase Diagrams, 2nd edition, ASM International, Metals Park, OH, 1990.
[2] O. Kubaschewski, Iron-Binary Phase Diagrams, Springer Verlag, Berlin, 1982.
[3] B. Hallemans, P. Wollants, J.R. Roos, Z. Metallkd. 85 (1994) 676.
[4] L. Kaufman, B. Uhrenius, D. Birnie, K. Taylor, CALPHAD 8 (1984) 25.
[5] M. Yukinobu, O. Ogawa, S. Goto, Metall Trans. B 20B (1989) 705.
[6] X. Huang, W.G. Ischak, H. Fukuyama, T. Fujisawa, C. Yamauchi, Tetsu-to Hagané 81 (1995) 1049.
[7] H. Ohtani, M. Hasebe, K. Ishida, T. Nishizawa, Trans. ISIJ 28 (1988) 1043.
[8] W. Obrowski, Nqaturwissenschqaften 48 (1961) 428.
[9] M. Kimoto, T. Itoh, T. Nagasaka, M. Hino, ISIJ Int. 42 (2002) 23.
[10] M.W. Chase (Ed.), NIST-JANAF Thermochemical Tables, 4th edition, American Institute of Physics, NY, 1998.
[11] H. Schenck, M.G. Frohberg, E. Steinmetz, B. Rutenberg, Arch. Eisenhüttenwes. 33 (1962) 223.
[12] D.L. Ball, Trans. Met. Soc. AIME 239 (1967) 31.
[13] D.B. Evans, R.D. Pehlke, Trans. Met. Soc. AIME 230 (1964) 1657.
[14] R.J. Fruehan, Met. Trans. 1 (1970) 2083.
[15] J.F. Elliott, M. Gleiser, V. Ramakrishna (Eds.), Thermochemistry of Steelmaking, vol. 1, Addison-Wesley Pub. Co. Inc., 1963.
[16] C. Ji, R. Yu, S. Liu, Can. Metall. Q. 27 (1988) 41.
[17] M. Hillert, L.-I. Staffanson, Acta Chem. Scand. 24 (1970) 3618.
[18] N. Saunders, A.P. Miodownik, Calphad (Calculation of Phase Diagrams.) A Comprehensive Guide, Pergamon, Oxford, 1988, p. 91.
[19] H. Ohtani, M. Hasebe, T. Nishizawa, Trans. ISIJ 24 (1984) 857.
[20] I. Ansara, A.T. Dinsdale, M.H. Rand (Eds.), COST 507, in: The Thermochemical Database for Light Metal Alloys, vol. 2, Office for Official Publications of European Communities, Luxembourg, 1998.